Revista Mexicana de Astronomía y Astrofísica
Universidad Nacional Autónoma de México
rmaa@astroscu.unam.mx
ISSN (Versión impresa): 0185-1101
MÉXICO

2001
W. J. Schuster / L. Parrao
THE ATMOSPHERIC EXTINCTION OF SAN PEDRO MÁRTIR W. J. SCHUSTER & L. PARRAO
Revista Mexicana de Astronomía y Astrofísica, octubre, año/vol. 37, número 002
Universidad Nacional Autónoma de México
Distrito Federal, México
pp. 187-200

Revista Mexicana de Astronomía y Astrofísica, **37**, 187–200 (2001)

THE ATMOSPHERIC EXTINCTION OF SAN PEDRO MÁRTIR[1]

W. J. Schuster[2] and L. Parrao[3]

Received 2001 April 6; accepted 2001 July 9

RESUMEN

Se analiza la extinción atmosférica de San Pedro Mártir (SPM) utilizando determinaciones en 13 colores de 294 noches de observación durante los años de 1973–1983, además de mediciones de extinción para 272 noches de observación en *uvby* durante los años 1984–1999. Se obtiene el comportamiento general de la extinción normal en SPM, y se analiza éste como función de la longitud de onda y del tiempo; se aportan valores promedio y mínimos para esta extinción. La extinción atmosférica promedio en SPM, excluyendo erupciones volcánicas, no cambió apreciablemente durante el período 1973–1999. Se presenta un modelo sencillo, de tres componentes, para la extinción en SPM. Los aerosoles normales, promedio, no volcánicos sobre SPM se ajustan bien por $k_p(\lambda) = 0.0254(\lambda)^{-0.87}$. Se presentan las determinaciones de la extinción para los períodos que siguieron a las erupciones de los volcanes de El Chichón y el Pinatubo: los datos en 13 colores muestran los efectos de El Chichón, y los datos *uvby* los del Pinatubo. Se analizan las curvas de extinción y sus variaciones para estudiar los aerosoles volcánicos y su evolución en el tiempo. Se estudia también la temporada de observación de abril y mayo de 1998, en la cual ocurrieron grandes variaciones no volcánicas en la extinción, y se presentan deducciones sobre estos aerosoles inusuales.

ABSTRACT

The atmospheric extinction of San Pedro Mártir (SPM) is analyzed using 13-color determinations from 294 nights of observations over the years 1973–1983, plus the extinction measures from 272 nights of *uvby* observations over the years 1984–1999. The general behavior of the normal extinction at SPM is given and analyzed as a function of wavelength and as a function of time. The average atmospheric extinction at SPM, excluding volcanic outbursts, has not changed significantly over the period 1973–1999. A simple 3-component model for the extinction above SPM is derived and presented; the normal, average, non-volcanic aerosols above SPM are well fit by $k_{\rm p}(\lambda) = 0.0254\lambda^{-0.87}$. The extinction determinations for the periods following the volcanoes El Chichón and Pinatubo are given: 13C data show the effects of El Chichón and *uvby* for Pinatubo. The extinction curves and their variations are analyzed to study the volcanic aerosols and their evolution with time. The Apr/May'98 observing run, when large non-volcanic extinction variations occurred, is also studied and deductions drawn concerning these unusual aerosols.

Key Words: **ATMOSPHERIC EXTINCTION — ATMOSPHERES: TERRESTRIAL — TECHNIQUES: PHOTOMETRIC**

[1]Based on observations collected at the Observatorio Astronómico Nacional at San Pedro Mártir, Baja California, México.

[2]Instituto de Astronomía and Observatorio Astronómico Nacional, UNAM, Ensenada, B. C.

[3]Instituto de Astronomía, Universidad Nacional Autónoma de México.

1. INTRODUCTION

Since its beginnings in 1968, stellar photometry has played a very important role in the development of the Mexican National Astronomical Observatory at San Pedro Mártir, Baja California, México (hereafter SPM). Some of the very first astronomical equipment on this mountain were stellar photometers, such as one of the original Johnson UBVRI photometers and also the 13-color, 8C and 6RC, photometers of Johnson, Mitchell, & Latham (1967) and of Mitchell & Johnson (1970). Later the Lowell pulse counting photometers were acquired as well as rapid and dual-channel photometers. The "Danish" 6-channel *uvby-β* photometer arrived near the end of 1983 and has played a key part in many of the photometric programs at this observatory. Over the last few years CCD detectors have replaced in part these classical photometers for the observation of stellar objects, especially for extended ones such as open and globular clusters. However, much of the most precise, accurate, and well-calibrated stellar photometry is still being carried out at SPM with the classical photometers such as the "Danish". Several important projects and surveys have resulted, such as those concerning variable stars (González-Bedolla 1990), subdwarf, metal-poor and high-velocity stars (Schuster & Nissen 1988; Schuster, Parrao, & Contreras-Martínez 1993), and also pre-main-sequence objects (Chavarría et al. 1988; 2000).

The SPM observatory has been characterized in several previous publications, such as the preliminary report of Mendoza (1971), and the climatological and meteorological studies of Alvarez & Maisterrena (1977) and of Tapia (1992). Astronomical seeing at SPM has been evaluated in works by Walker (1971) and Echevarria et al. (1998). The precipitable water vapor above SPM has been determined and analyzed by Hiriart et al. (1997) and the turbulence profiles above the 1.5 m and 2.1 m telescopes by Avila, Vernin, & Cuevas (1998). Previous studies of the atmospheric extinction at SPM have been published by Schuster (1982), (hereafter S82) and by Schuster & Guichard (1985), (hereafter SG). In the former the 13-color photometric system was used to study the atmospheric extinction as a function of wavelength and of time. The extinction curve versus λ was given from 212 nights of normal observations, plus the curves from two special extinction nights observed to large air masses with the participation of M. Alvarez. Year to year variations, monthly averages and an overall mean were presented. The atmospheric extinction of SPM was compared to that of 23 other astronomical observatories, that of SPM being the second lowest, surpassed only by Mauna Kea, Hawaii. The extinction curve and its variations were assessed in terms of the wind and rainfall patterns of this observatory; northern winds, for example, bring higher extinctions due to urban and dust pollutants from the north. In SG more yearly means were given as well as the extinction curve versus wavelength for normal conditions and for the two years following the El Chichón volcano in 1982. Arguments were made for a possible bi-modal distribution of aerosols following this volcano, for the masking of the usual ozone absorption near 5800 Å, and for additional absorption at the 37 filter due to the SO_2 molecule.

In the present study the atmospheric extinction of SPM is reanalyzed using the 13-color (hereafter 13C) results from 294 nights of observations over the years 1973–1983, plus the extinction determinations from 272 nights of *uvby-β* observations over the years 1984–1999. In § 2 the observing techniques used for the extinction determinations are discussed briefly. In § 3 the general behavior of the normal extinction at SPM is given and analyzed as a function of wavelength and as a function of time. Mean and minimum atmospheric extinction values for SPM are given. In § 4 a simple 3-component model for the extinction above SPM is derived and presented; this model includes Rayleigh and aerosol scattering plus ozone absorption and fits the observed extinction curve well over 3370–6500 Å. In § 5 the extinction determinations for the periods following the volcanoes El Chichón and Pinatubo are given, 13C data for the effects of El Chichón and *uvby* for Pinatubo. The extinction changes and variations are analyzed to study the volcanic aerosols and their evolution with time, and to detect possible masking of the usual extinction components. The Apr/May'98 observing run, when large non-volcanic extinction variations occurred, is also studied, and deductions drawn concerning the climatological conditions and their unusual aerosols. Our conclusions are given in § 6.

2. OBSERVING TECHNIQUES

The 13C extinction determinations were made with the single-channel 8C and 6RC photometers described in S82 and SG. Briefly, the Bouguer method for the determination of the atmospheric extinction coefficients has been employed. Usually one extinction pair, including one red and one blue star, near the celestial equator, was observed three times, at small, intermediate, and large air masses. Infrequently, two extinction pairs were observed, each at small and large air masses. For each case an

air mass range of at least 0.8 was required for the extinction solution. Being single-channel photometers the observations were fairly slow, and so usually less than 15 standard stars (including the extinction stars) were observed per night. Although each extinction pair contained both a red and blue star, no second-order extinction terms were needed, except perhaps a very small one for the 33 filter, which has been ignored.

The 4-color extinction determinations were made using the *uvby-β*, 6-channel photometer on SPM at the 1.5 m H.L. Johnson telescope. More details concerning our observing techniques can be found in Schuster & Nissen (1988) and Grønbech, Olsen, & Strömgren (1976). Tests have shown that the second-order extinction term in c_1 is less than $0\overset{m}{.}002$, and so it has been ignored. So, extinction pairs have been retained here not for the second-order term but for the greater precision provided; these pairs usually contained F- and G-type standard stars, similar to our metal-poor program stars. Again they were located near the celestial equator for optimal efficiency and precision. The Bouguer method has again been used, and usually the air-mass range of the extinction determinations was greater than 0.8. If the pair was well centered during the night, it was observed 5 times: $\gtrsim$ 4.0 and 2.5–2.0 hours east of the meridian, then crossing the meridian, and finally 2.0–2.5 and $\gtrsim$ 4.0 hours west. If the pair was not so well centered, only four observations of the pair were obtained with a single observation at $\sim$ 3.0 hours substituted, east or west, depending on the centering.

All the observations were reduced using Fortran programs graciously provided by T. Andersen and P.E. Nissen, and these are documented in Parrao, Schuster, & Arellano-Ferro (1988) and follow closely the precepts of Grønbech et al. (1976). All nights of an observing run are reduced together to provide an instrumental photometric system. The output of the reduction provides nightly extinction coefficients together with their error estimates as well as the constant and temporal terms of the night correction for each night, as defined by Grønbech et al. (1976). The linear-time terms of the night corrections depend upon the observations of "drift" stars observed symmetrically east and west of the meridian; these are stars with more northerly declinations ($\gtrsim +20°$). Typical (median) estimated errors for the extinction coefficients of y, $(b-y)$, m_1, c_1 are $\pm$ 0.0030, 0.0016, 0.0025, and 0.0.0030. The program also outputs nightly scatters to help us evaluate the photometric quality of the nights.

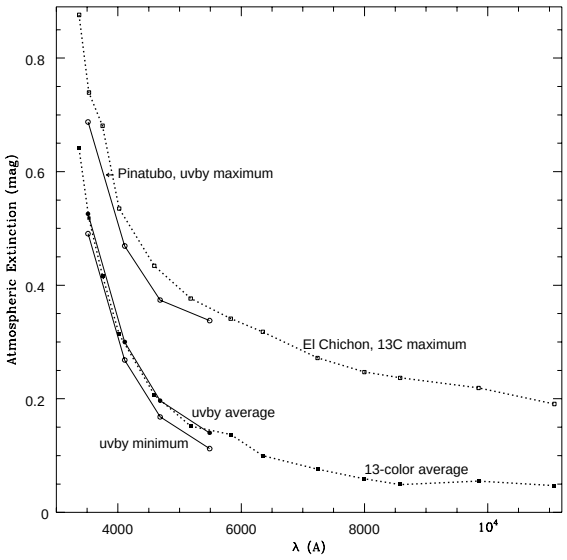

Fig. 1. Atmospheric extinction versus the equivalent wavelengths of the 13C and 4-color filters. Solid squares and circles show the average extinctions from 151(8C)/120(6RC) nights of 13C photometry and 158(mags.)/182(colors) nights of 4-color photometry, respectively. The lowest curve shows the "minimum" 4-color extinction as derived from 12 nights with optimal, stable conditions from 6 good observing runs from 1988 through 1998. These mean and minimum values are shown in Table 1. The highest curves of this graph show the maximum effects caused by volcanic aerosols, the night of 19/20 Jun'82 for 13C photometry and the El Chichón volcano (open squares), and the night of 4/5 May'92 for 4-colors and Pinatubo (open circles).

3. BEHAVIOR OF THE ATMOSPHERIC EXTINCTION AT SPM

3.1. *As a Function of Wavelength*

In Figure 1 are shown the mean and extreme atmospheric extinctions observed at SPM over the years 1973 through 1999 with the 13C and 4-color photometry. The extinction values are plotted versus the equivalent wavelengths of the photometric band passes. For 13C these wavelengths have been taken from Mitchell & Johnson (1970). For the 4-color photometry the equivalent wavelengths have been taken from the manual of Nissen (1984) with a small correction to the "u" wavelength according to the new atmospheric extinction model of this paper (see § 4 below). For 4-color photometry the equivalent wavelengths used here are: 3515, 4110, 4685, and 5488 Å. Fig. 1 shows the mean 13C extinction curve for 271 nights of 8C and 6RC photometry over

the years 1973–1981, prior to the El Chichón volcano and its strong effects on the atmospheric extinction. 151 nights of 8C and 120 of 6RC photometry go into this average 13C curve. Also shown is the mean 4-color extinction curve for the period 1984–1999 with the observations from Oct'91 through Apr'94 omitted due to the effects of the Pinatubo volcano. For this "*uvby* average" curve 182 nights define the shape of the curve while only 158 nights the level. As discussed in Schuster & Nissen (1988) a small subset of our observations have been made through light cirrus clouds in the absence of moonlight; observations made with the simultaneous multichannel photometer provide good color and index data through light clouds, but not good magnitudes. Also plotted in Fig. 1 is a "*uvby* minimum" curve which represents the average of 12 nights with the lowest extinction determinations from six observing runs with the lowest average extinctions and most stable observing conditions: Jun'88, Nov'89, Oct'94, Oct'97, Nov'97, and Nov'98. The average of 12 nights is given here to present a value which is robust and representative.

In Table 1 are shown the mean and minimum extinction coefficients observed at SPM for the 13C and 4-color photometry as shown in Fig. 1; for the 4-color results both the observed color and index extinctions are given with their dispersions (of a single measure), as well as the extinctions converted to magnitude values. The "mean" four-color values exclude the dates affected by Pinatubo, and the "minimum" values use the 12 nights from the 6 stable observing runs mentioned above. The 13-color averages cover the years 1973–1981.

Also plotted in Fig. 1 are the most extreme extinctions observed at SPM by us using the 13C and 4-color photometers. The 13C maximum occurred for the period following the El Chichón volcanic eruption. The level and blue part of this curve are defined by a single night, the 19/20th of Jun'82, while the red part of this curve includes 6RC data from several nights during 1982 following the eruption. The "*uvby* maximum" curve comes from the observations of a single night, 4/5 May'92, during the maximum effects at SPM due to the Pinatubo volcano.

The average 13C extinction curve of Fig. 1 shows the expected shape over the wavelength range 3370–11,080 Å with Rayleigh and aerosol scattering plus ozone absorption dominating over 3370–6500 Å and additional absorptions by O_2 and H_2O for $\lambda \gtrsim 6500$ Å (Cox 2000, Fig. 11-4). Also this 13C curve of Fig. 1 shows a bump at the 58 filter which is probably evidence for the Chappuis bands of ozone; the strongest absorptions of the Chappuis bands occur over the wavelengths 5650–6250 Å (Gast 1961) . The two "average" curves of Fig. 1 are in very good agreement indicating that the mean atmospheric extinction of SPM has not evolved significantly, outside of the volcanic episodes, from the 1973–1981 period through 1984–1999. For example, the mean visual extinction (filters 52 and 58) from 13C was $0\overset{m}{.}144$ per air mass from 151 nights of 8C observations and $0\overset{m}{.}140$ per air mass from 158 nights of 4-color determinations. The "minimum" curve shows $k_V \sim 0\overset{m}{.}11$ per air mass, which compares very favorably with that of many other observatories (S82); Burki et al. (1995), (hereafter B95) obtained a minimum of $k_V \sim 0\overset{m}{.}13$ from about 4,400 nights of photometry at the La Silla, Chile, observatory using the seven bands of the Geneva photometric system.

TABLE 1

OBSERVED EXTINCTION AT SPM

Four Color

Color:	y	$(b-y)$	m_1	c_1	N
Mean	+0.140 ±0.030	+0.057 ±0.006	+0.047 ±0.008	+0.122 ±0.009	158/182
Min	+0.112 ±0.002	+0.056 ±0.004	+0.044 ±0.007	+0.122 ±0.010	12

Filter:	u	v	b	y	N
Mean	0.526	0.300	0.197	0.140	158/182
Min	0.491	0.268	0.168	0.112	12

13-Color

Filter	33	35	37	40	N(8C)	
Mean	0.641	0.518	0.417	0.314	151	
Filter	45	52	58	63	N(8C)	
Mean	0.207	0.152	0.137	0.100	151	
Filter	72	80	86	99	110	N(6RC)
Mean	0.076	0.059	0.049	0.055	0.047	120

The two extreme curves of Fig. 1 show similar levels for the two volcanoes. These extrema also give us the first indications for the differing and unusual wavelength dependences for the volcanic aerosols (see § 5 below); the El Chichón curve has an upward shift from the mean of $0\overset{m}{.}221$ in the ultraviolet (filter 35) and $0\overset{m}{.}214$ in the visible (filters 52 and 58), while the Pinatubo curve is displaced $0\overset{m}{.}162$ and $0\overset{m}{.}198$ in the UV and visible, respectively.

3.2. *As a Function of Time*

Figure 2 shows the variation of k_y at SPM from the end of 1984 through 1999, determined with the *uvby-β* photometer. In the upper graph the average values plus error bars are shown for 33 different observing runs, as a function of the civil calendar; in the middle panel the k_y values are plotted for nightly values as a function of the Julian date. The triangles show our extinction values as measured according to the methods and techniques discussed in § 2. The filled squares show extinction data measured and graciously provided by other observers, such as S. González-Bedolla, A. Ruelas-Mayorga, J. H. Peña, and A. Arellano-Ferro; these are plotted here for completeness and better coverage, but are not used for the modeling and analyses to follow due to the differing observing and reduction methods employed. The upper horizontal bar marks the interval of observations affected by the volcanic aerosols from Pinatubo, Julian dates about 2448400–9500, including the Oct'91, Mar'92, Apr/May'92, Nov'92, Mar'93, May'93, Sep'93, Nov'93, and Apr'94 observing runs. Large variations and instability are also noted for the Apr/May'98 observing run (and also for Feb'85 and May'89), not caused by any volcanic activity; this behavior will be discussed in § 5.3.

In the lower panel of Fig. 2 five expanded plots are shown for five of the observing runs; four of these, Oct'91, Mar'92, Apr/May'92, and Nov'92, were clearly affected by the Pinatubo aerosols, and the fifth, the first run of the Apr/May'98 period, was extinguished by some sort of significant non-volcanic absorption. The Pinatubo plots, especially the ones for Oct'91 and Apr/May'92, show evidence for the striations and patchiness of the volcanic aerosols as has been detected and discussed in other works, such as Stothers (2001). On the other hand, the expanded plot for the Apr/May'98 run shows clear evidence for a single event or aerosol cloud having passed over SPM, with its maximum effect happening during the night of 26/27 Apr'98.

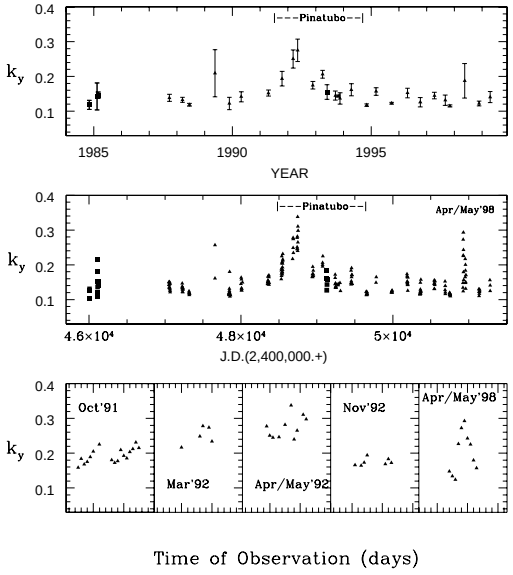

Fig. 2. In the upper panel the average atmospheric extinction values for the "*y*" band are plotted with their dispersions as a function of the civil calendar for 33 observing runs from Oct'84 through Apr'99. The interval probably affected by the volcanic aerosols from Pinatubo is indicated. Triangles show values measured by us, while filled squares values measured by others. The middle panel shows the same, but for the nightly individual values, as a function of the Julian dates. The Apr/May'98 period, which showed a large, non-volcanic variation in the atmospheric extinction, is also labeled. The bottom panel displays expanded plots for five of the observing runs, four affected by the Pinatubo aerosols and the first observing run of the Apr/May'98 period.

In Figure 3 the extinction coefficients for y, $(b-y)$, m_1, and c_1 are plotted as a function of the month of the year. The data affected by Pinatubo have been excluded. It can be seen that the larger extinction excursions for SPM generally occur for the spring months of March–May while the fall months are more stable; this had been noted by S82 from 13C extinction data. This latter result can also be appreciated from the list of observing runs used for the "minimum" curve of Fig. 1; five out of six were in October or November. This Fig. 3 can be contrasted with Figure 6 of B95 where the largest extinction excursions happen at La Silla during the southern summer months; during the summer the reversing layer is sometimes above La Silla. The explanation for SPM is not so obvious. According to Tapia (1992), May is the month with the highest percentage of photometric nights at SPM, while April and May are the two months with the highest percentages of

nights with high relative humidity. Large meteorological aerosols, i.e., "haze" (water droplets), may have caused the higher atmospheric extinctions. On SPM the costal or local inversion layers probably do not reverse or break down during such episodes (Alvarez & Maisterrena 1977). And, as the discussion of § 5.3 shows, wind direction may also play an important role. It is curious that Echevarría et al. (1998) obtained better seeing results at SPM for the spring and summer months and poorer for the autumn and winter; perhaps the higher humidities of the spring (Tapia 1992) promote better seeing but at the same time larger meteorological aerosols with higher and less stable atmospheric extinctions. More complete meteorological data are needed for SPM.

4. A THREE-COMPONENT MODEL FOR THE ATMOSPHERIC EXTINCTION OF SPM.

4.1. *The Model*

The atmospheric extinction model developed in this section follows closely the physics and formulism given in papers such as B95, Gutiérrez-Moreno, Moreno, & Cortés (1982), and Hayes & Latham (1975). It assumes that the extinction over $3200 \lesssim \lambda \lesssim 6500$ Å can be represented by three independent contributions due to Rayleigh-Cabannes and aerosol scatterings and ozone absorption

$$\begin{aligned} k(\lambda) &= k_{\rm p}(\lambda) + k_{\rm RC}(\lambda) + k_{\rm O_3}(\lambda), \\ &= a\lambda^{-\alpha_{\rm p}} + b\lambda^{-4.05} + ck_{\rm oz}(\lambda), \end{aligned} \qquad (1)$$

where $k_{\rm p}(\lambda)$ represents the aerosol term given by $a\lambda^{-\alpha_{\rm p}}$; $k_{RC}(\lambda)$ is the Rayleigh-Cabannes component given by $b\lambda^{-4.05}$, where the exponent of -4.05 has been taken from Allen (1973) and includes approximately the refractive effects; and $k_{\rm O_3}(\lambda)$, the ozone contribution given by $ck_{\rm oz}(\lambda)$. For the normalization of this model, the Rayleigh-Cabannes coefficient "b" is calculated to be 0.0067 according to equation (1) of Hayes & Latham (1975), using an altitude of 2790 m for the 1.5 m telescope on SPM and assuming a density scale height of 7.996 km for the lower troposphere (Hayes & Latham 1975). This normalization corresponds to standard conditions, and variations in barometric pressure may cause uncertainties of about one percent. For the ozone term, equation (2) of Hayes & Latham (1975) has been adapted so that $c = 1.11\ T_{\rm oz}$ where $T_{\rm oz}$ can be taken from § 59 of Allen (1963) according to the latitude of SPM and according to the months when most of our observations were taken. We find $T_{\rm oz} \sim 0.2325$ giving $c \sim 0.2581$. The values of $k_{\rm oz}(\lambda)$ can be obtained from Gast (1961), (Tables 16–16B and 16–16C) by convolving his ozone data with the filter sensitivity functions, from Grønbech et al. (1976) for the *uvby* system and from Johnson et al. (1967) and Mitchell & Johnson (1970) for 13C. The ozone data (Gast 1961) given for a temperature of $-44°C$ were used whenever possible corresponding to altitudes of 10 to 35 km, where most of the pertinent atmospheric ozone is concentrated. Since the ozone absorption can be quite variable (Hayes & Latham 1975), these ozone extinction values provide us only with the means of studying the average atmospheric extinction above SPM.

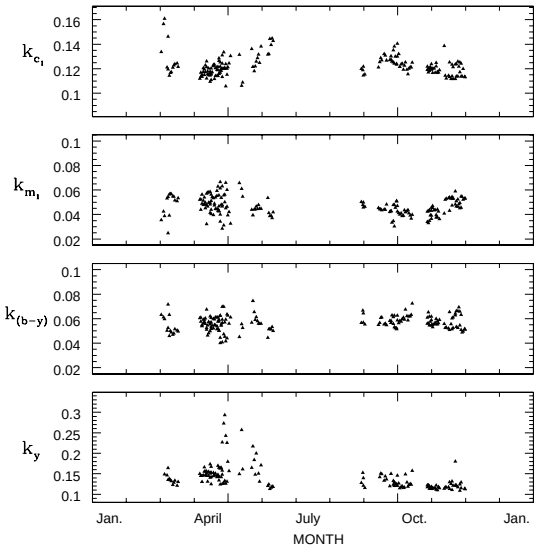

Fig. 3. The atmospheric extinctions for c_1, m_1, $(b-y)$, and y are plotted versus the months of their observation in order to detect and study the seasonal and annual variations. The data affected by the aerosols from the Pinatubo volcano have been removed from this plot.

The aerosol contribution can now be studied by subtracting the Rayleigh-Cabannes and ozone extinctions from the total observed extinction

$$k_{\rm p}(\lambda) = k(\lambda) - k_{\rm RC}(\lambda) - k_{\rm O_3}(\lambda) = a\lambda^{-\alpha_{\rm p}}. \qquad (2)$$

This equation must now be solved for a and $-\alpha_{\rm p}$ using our observed mean extinction data. A method similar to that of B95 is used here for our 4-color data. Regressions of $k_{\rm p}(\lambda_{\rm u})$, $k_{\rm p}(\lambda_{\rm v})$, and $k_{\rm p}(\lambda_{\rm y})$ against $k_{\rm p}(\lambda_{\rm b})$ have been made, with the mean minimum extinctions of Table 1 subtracted; these relations are shown in Figure 4. Here we are mainly concerned with normal, average conditions above SPM, and so the data affected by Pinatubo and the data of the unstable observing runs such as May'89 and Apr/May'98 have been removed from

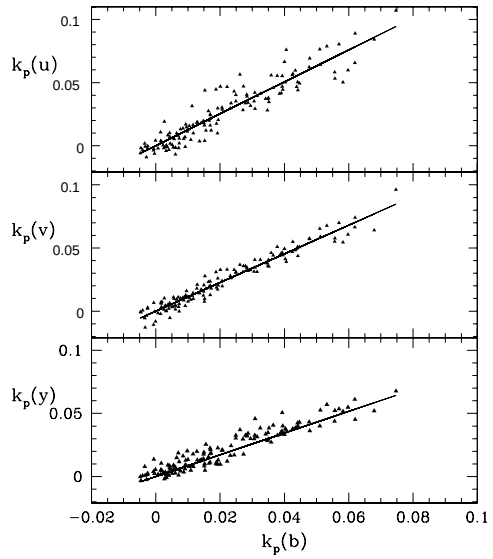

Fig. 4. The $k_{\rm p}(u)$, $k_{\rm p}(v)$, and $k_{\rm p}(y)$ versus $k_{\rm p}(b)$ plots for 138 nights of extinction data. Data affected by Pinatubo and data from the less stable Apr/May'98 and May'89 observing runs have been removed. Regressions to this data give the extinction ratios to be used in the $log[k_{\rm p}(\lambda_{\rm i})/k_{\rm p}(\lambda_{\rm b})]$ versus $log[\lambda_{\rm i}/\lambda_{\rm b}]$ method as discussed in the text and shown in the following graph. The regressions shown here have slopes of 1.265 for $k_{\rm p}(u)$, 1.134 for $k_{\rm p}(v)$, and 0.861 for $k_{\rm p}(y)$.

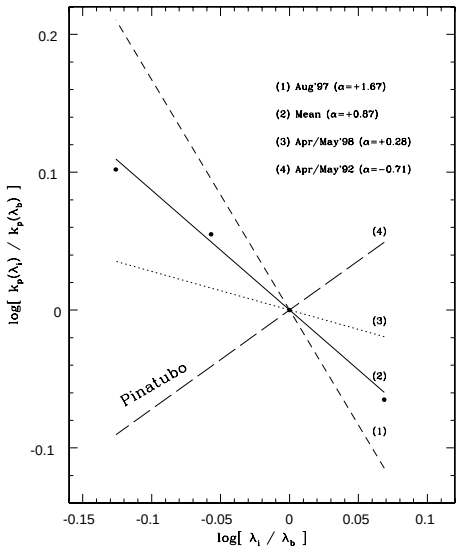

Fig. 5. The $log[k_{\rm p}(\lambda_{\rm i})/k_{\rm p}(\lambda_{\rm b})$ versus $log[\lambda_{\rm i}/\lambda_{\rm b}]$ graph for determining the $\alpha_{\rm p}$ exponent of the normal, average aerosol extinction above SPM. The regression which is shown by filled circles corresponds to the slopes of Fig. 4 and gives $\alpha_{\rm p} = 0.87 \pm 0.04$, so that the extinction law for the average, normal aerosols is of the form $k_{\rm p}(\lambda) = a\lambda^{-0.87}$. Also shown is the slope for the most negative $\alpha_{\rm p}$ found during the Apr/May'92 observing run, which was hightly affected by the Pinatubo volcanic aerosols (see Fig. 9 below); the nearly neutral slope obtained during the Apr/May'98 run ($+0.28 \pm 0.04$), discussed in § 5.3; and the curve with the most positive $\alpha_{\rm p}$ ($+1.67 \pm 0.04$), for the Aug'97 observations, indicating some of the smallest aerosol particles above SPM.

the analyses leaving 138 nights of *uvby* data. The results of these regressions are then plotted in the form, $log[k_{\rm p}(\lambda_{\rm i})/k_{\rm p}(\lambda_{\rm b})]$ versus $log[\lambda_{\rm i}/\lambda_{\rm b}]$, as shown in Figure 5. A regression of this graph then gives $\alpha_{\rm p}$. For normal, average conditions on SPM, $\alpha_{\rm p} = 0.87 \pm 0.04$ is obtained. Then equation (2) can be used to derive the turbidity factor "a". For 13C the filters 33 through 63 give, $< a >_{33-63} = 0.02524 \pm 0.00308$; the 13C filters 72 through 110 are not used here since they are probably affected by other absorption components (Cox 2000). For the 4-color results the "u" calculation does not agree that well with the values from "*vby*", probably due to still some uncertainty in its equivalent wavelength, which is magnified by the steeply increasing Rayleigh-Cabannes dispersion for this filter. The other three 4-color measures of extinction give, $< a >= 0.02547 \pm 0.00020$, which agrees well with the 13C result. Inverting the process would imply an equivalent wavelength for the "u" band of 3533 Å, as compared to our given 3515 Å, the difference being well within this band's uncertainty. So the normal mean aerosols above SPM can be represented by

$$k_{\rm p}(\lambda) = a\lambda^{-\alpha_{\rm p}} = 0.0254\lambda^{-0.87},$$

and our total model by

$$k(\lambda) = 0.0254\lambda^{-0.87} + 0.0067\lambda^{-4.05} + 0.2581k_{\rm oz}(\lambda), \quad (3)$$

where λ is measured in microns. In Table 2 are presented the extinction values for these three components, plus the summed model and observed extinctions, for the 4-color and 13C photometry.

In Figures 6 and 7 are shown the components of our 3-component model for the atmospheric extinction over SPM and the fits of this model to our mean extinctions for the 13C and 4-color photometry. The upper panel of Fig. 6 shows the individual contributions of Rayleigh and aerosol scatterings and ozone absorption within the bands of the 13C system, plus the observed mean extinction for 13C and the model shifted upward by 0.05 for comparison. The lower panel shows the fit of the model to the observed

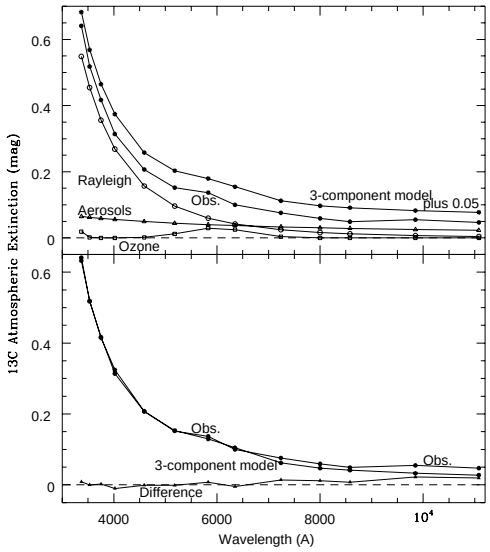

Fig. 6. The upper panel of this figure shows the three components of our simple extinction model for SPM in the 13C photometric system, plus the mean 13C extinction of SPM from Table 1, and finally the sum of the three components shifted upward by 0.05 for clarity and comparison. Open squares represent the ozone contribution for SPM, open triangles the aerosol contribution, open circles the Rayleigh-Cabannes, filled circles the mean observed extinction, and asterisks the shifted model. In the lower panel the observed-mean and model extinctions are over-plotted, and below the residuals (obs.−model) are plotted as filled triangles, all as a function of the equivalent wavelengths of the 13C filters. The model fits the observed curve very well for 3700–6500 Å but falls short for greater wavelengths due to the lack of absorptions by O_2 and by H_2O.

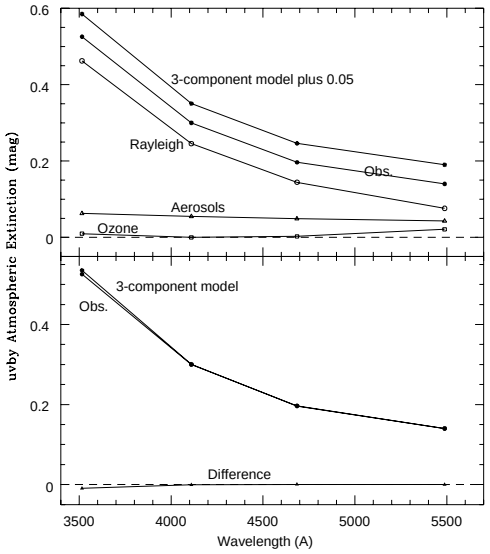

Fig. 7. The same as Fig. 6, but for the 4-color, *uvby*, photometric system.

mean extinction, and at the bottom the residuals of this fit, all as a function of the equivalent wavelengths. Fig. 7 shows the same for the 4-color system and its mean atmospheric extinction above SPM. The mean residual of the lower panel of Fig. 6 is $< \Delta_{\rm obs-model} >= -0\overset{\rm m}{.}0002 \pm 0\overset{\rm m}{.}0061$ for the fit of the filters 33 through 63, using $a = 0.0254$, and for the lower part of Fig. 7 for 4-colors, $< \Delta_{\rm obs-model} >= -0\overset{\rm m}{.}0022 \pm 0\overset{\rm m}{.}0047$, including all four bands. The mean residual of Fig. 7 for the "*vby*" bands is $< \Delta_{\rm obs-model} >= +0\overset{\rm m}{.}0001 \pm 0\overset{\rm m}{.}0004$. In Fig. 6 it can be seen that the 3-component model falls short for wavelengths greater than 6500 Å, for the filters 72 through 110. This is what one would expect from the data plotted in Fig. 11-4 of Cox (2000); there are additional absorptions by O_2 and by H_2O for these longer wavelengths, and so our 3-component model is no longer complete.

4.2. *Comparisons with other Observatories*

Our value for the exponent of the aerosol scattering can be compared to that for other observatories. For example, B95 obtain $k_{\rm p}(\lambda) = a\lambda^{-1.39}$ for La Silla, Chile, from about 4,400 nights using the Geneva photometric system, and they comment that values close to this, -1.3 ± 0.2, are found "...at a large variety of locations on the Earth... being seldom above -0.5 or below -1.6." However, Gutiérrez-Moreno et al. (1982) find values of $\alpha_{\rm p}$ varying from 0.2 to 2.6 from a large data set of monochromatic extinction determinations made at the Cerro Tololo Inter-American Observatory, Chile, from 1964 to 1980. Hayes & Latham (1975) find values from 0.49 to 0.89 for stellar observations at several observatories, such as Le Houga, Boyden, Lick, Cerro Tololo, and Mount Hopkins. They find a mean weighted value of 0.81 for their stellar observations and adopt $\alpha_{\rm p} = 0.8$ for nighttime stellar photometry, very close to the value that we have obtained for SPM. They comment, "this value is smaller than those quoted in the literature on atmospheric aerosols, which usually refer to lower altitudes and poorer transparency conditions, such as are found near urban centers."

As discussed in many of the above references, this aerosol exponent is closely related to the sizes

TABLE 2

MODEL FOR SPM MEAN EXTINCTION

Filter	$k_{\rm p}$	$k_{\rm RC}$	$k_{\rm O_3}$	Model	Observed
33	0.065	0.548	0.0193	0.632	0.641
35	0.063	0.455	0.0015	0.520	0.518
37	0.059	0.356	0.0000	0.415	0.417
40	0.056	0.269	0.0001	0.325	0.314
45	0.050	0.157	0.0015	0.208	0.207
52	0.045	0.096	0.0124	0.153	0.152
58	0.041	0.060	0.0295	0.130	0.137
63	0.038	0.042	0.0250	0.105	0.100
72	0.034	0.025	0.0039	0.063	0.076
80	0.031	0.016	0.0000	0.047	0.059
86	0.029	0.012	0.0000	0.041	0.049
99	0.026	0.007	0.0000	0.033	0.055
110	0.023	0.004	0.0000	0.027	0.047
u	0.063	0.462	0.0097	0.535	0.526
v	0.055	0.245	0.0000	0.300	0.300
b	0.049	0.144	0.0028	0.196	0.197
y	0.043	0.076	0.0212	0.140	0.140

of the particles producing the scattering, being of the order one for particles close in size to the wavelength of light at which the observations are made, closer to two for smaller particles, and less than one when these particles are much larger than the wavelength. Also, Gutiérrez-Moreno et al. (1982) find a relation between the amount of aerosol absorption (the turbidity factor), the "a" of our equations, and the value for $\alpha_{\rm p}$, with larger $\alpha_{\rm p}$ corresponding to smaller a and vice versa. This can be understood simply, that larger particles produce more total extinction than smaller particles due to their size and efficiency. Comparing our results, for example, to those of B95, we would conclude that the aerosol scattering of SPM, the meteorological "haze", is due to larger particles than those of La Silla, and the amount of aerosol scattering somewhat larger, although the minimum overall extinction of SPM is smaller than that of La Silla. In fact, Rufener (1986) found the very low value of 0.006 for the aerosol turbidity at La Silla, while we have found a more typical value of $a = 0.0254$ for SPM.

5. VOLCANOES AND OTHER ANOMALIES

5.1. *El Chichón*

The volcano El Chichón suffered two eruptions in México during 1982, March 23 and April 04, and 13C extinction measures were obtained at SPM soon after from three 8C and ten 6RC nights of observation mostly during Jun'82. Approximately one year later extinction determinations were obtained during seven 8C and three 6RC nights during Apr'83. In the upper panel of Figure 8 the mean 13C extinction curve from Table 1 is plotted as well as the curves from Jun'82 and Apr'83, where the effects of the El Chichón aerosols can be clearly seen. In the highest curve some details can be noticed which have been mostly explained by SG. For example, the extra small hump at the 37 filter is most probably due to absorptions by the SO_2 molecule which formed in abundance in the initial gas cloud of El Chichón (Krueger 1983). Also, the usual bump at the filter 58, probably due to the Chappuis bands of ozone, is not seen indicating masking by the strong volcanic aerosol presence.

To estimate the $\alpha_{\rm p}$ of the volcanic aerosols and thereby get an idea of the particle sizes, the method of Sterken & Manfroid (1992) has been applied, whereby the logarithmic shift of the extinction curve with respect to the normal mean extinction curve of Table 1 is plotted versus the logarithm of the equivalent wavelengths, as shown in the lower panel of Fig. 8, $ln[\Delta(extinction)]$ versus $ln[\lambda]$. The slope of the curve in such plots provides a measure of $\alpha_{\rm p}$. The Jun'82 curve is mostly flat for filters 33 through 52 (except for the peak at 37, as mentioned above) and then slopes down to the 110 filter. A regression to all points would estimate $\alpha_{\rm p} \sim +0.52$ while the seven reddest points, filters 58 through 110, give $\alpha_{\rm p} \sim +0.89$. These values and the shapes of the graphs would indicate particle sizes $\gtrsim 0.5$ μm in agreement with the discussion of SG for a bi-modal size distribution with sizes both larger and smaller than the typical pre-eruption sizes; the larger sizes detected here (radii near 0.5–0.7 μm) formed from the original pre-eruption aerosols by the accretion of sulfuric acid vapor.

The lower curve of the lower panel of Fig. 8 shows the logarithmic difference curve for Apr'83, approximately one year later. A regression of all points gives a negative $\alpha_{\rm p}$, -0.22, while the ten reddest points of the extinction curve (filters 40 through 110) give a nearly flat slope, $\alpha_{\rm p} \sim +0.03$. These values indicate even larger particle sizes, i.e. an evolution and growth of the volcanic aerosols with time, similar to the results for El Chichón of B95, but contrasting

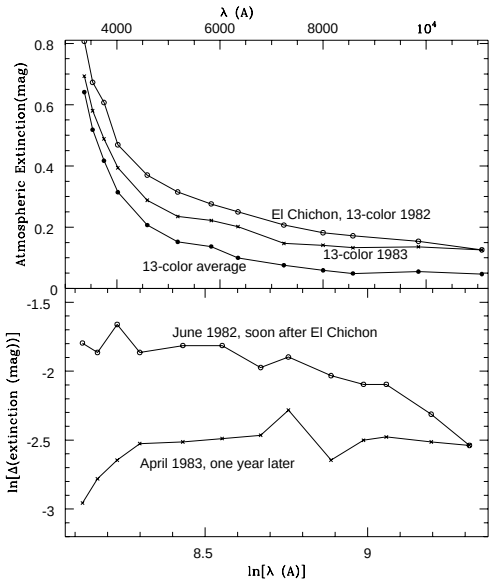

Fig. 8. 13C extinction data are plotted versus the equivalent wavelengths for data affected by volcanic aerosols from El Chichón. In the upper panel open circles show the mean values from three 8C and ten 6RC nights observed mostly during Jun'82 shortly after the volcano erupted, the X's mean values from seven 8C and three 6RC nights during Apr'83 approximately one year later, and beneath these curves the filled circles show the 13C mean extinction for SPM from Table 1. These extinction curves are plotted versus the equivalent wavelengths of the 13C system. In the lower panel of this figure the logarithmic shifts of these El Chichón extinction curves with respect to the normal mean extinction curve of Table 1 are plotted versus the logarithms of the equivalent wavelengths. These log-log plots can be used to measure the $\alpha_{\rm p}$ values of the extinction law produced by the volcanic aerosols and thereby estimate the particle sizes.

with the compilation of Stothers (1997), who found a "near constancy", sizes of 0.2–0.3 μm for about two years; perhaps we and Stothers' sources are measuring different components of a bi-modal size distribution. Our 13C results for El Chichón are very similar to those of B95; our $\alpha_{\rm p}$ value from Jun'82 is slightly less than their value from Jul'82 (0.85), but both find very flat extinction curves for the volcanic aerosols of Apr'83 with $\alpha_{\rm p}$'s very near zero. Also in the lower panel of Fig. 8 a sharp downturn is noted in the UV, for filters 33, 35, and 37; this may be further evidence for a masking or decrease of the normal atmospheric opacity caused by the strong presence of the volcanic aerosols, as discussed by Sterken & Manfroid (1992). In this case the atmospheric component most strongly masked would have to be the Rayleigh-Cabannes scattering because of the strong UV dependence of the downturn. Sterken & Manfroid (1992) invoked such masking as a possible explanation for the negative $\alpha_{\rm p}$ found for some volcanic aerosols, as will be discussed below for Pinatubo.

More recently Stothers (2001) has used our 13C data from 1982 and 1983 plus Mie scattering theory with the assumptions of a spherical particle shape, a lognormal distribution of particle radii, and an aerosol composition of 75% H_2SO_4 and 25% H_2O to obtain more quantitative estimates for the aerosol particle sizes. His newer results agree well with our conclusion that the particle sizes have grown from 1982 to 1983, but his estimates for the actual sizes are somewhat smaller. For the Jun'82, 13C data he derives an effective radius of 0.36 μm, and for Apr'83, 0.51 μm. But, this sort of difference for the size determinations is to be expected between Mie-scattering analyses with a lognormal assumption and rough size estimates based only upon the shape of the extinction curve (Stothers 2001).

5.2. *Pinatubo*

This volcano also had two main eruptions, on June 12 and 15 of 1991, and atmospheric extinction determinations were obtained at SPM in 4-colors during nine observing runs that were probably affected by the volcanic aerosols: Oct'91, Mar'92, Apr/May'92, Nov'92, Mar'93, May'93, Sep'93, Nov'93, and Apr'94. At La Silla, Chile, B95 found more than twice the effect from the Pinatubo aerosols than from those of El Chichón, while the two extrema of Fig. 1 show similar levels at SPM. Also, B95 concluded that the effects of this volcano upon the atmospheric extinction at La Silla continued for approximately 1000 days after the eruption, perhaps as long as 1300 days. In Fig. 2 the effects of Pinatubo at SPM probably lasted through Apr'94, for more than 900 days; by Oct'94 the mean atmospheric extinction had returned to its pre-eruption values. Enough 4-color extinction determinations were obtained by us at SPM to attempt an analysis of the volcanic aerosols by the two methods discussed above, the $\log[k_{\rm p}(\lambda_{\rm i})/k_{\rm p}(\lambda_{\rm b})]$ versus $\log[\lambda_{\rm i}/\lambda_{\rm b}]$ method, which was used above to characterize the normal aerosols above SPM, and also the $\ln[\Delta(\text{extinction})]$ versus $\ln[\lambda]$ method, used above to analyze the El Chichón aerosols. The first method gives us information mainly about the aerosol component which is varying during an observing run, (see Fig. 4) while the second method includes information about the aerosol component which produces the overall, more constant displacement of the extinction above the mean curve of Table 1. So,

TABLE 3

AEROSOL EXPONENT FOR PINATUBO CLOUD

Date		α from		Notes
		$log[\frac{k_p(\lambda_i)}{k_p(\lambda_b)}]$	$\ln(\Delta k)$	
October	1991	+0.05	+0.00	
March	1992	−0.30	−0.39	
April/May	1992	−0.71	−0.32	
May 5	1992	....	−0.41	Single night maximum
November	1992	+0.27	....	
March	1993	+0.94	−0.48	
September	1993	+1.60	....	
April	1994	+0.78	....	Return to normal?

this second method measures the aerosol component which is more persistent during the observing run, apart from the variable component. These two methods may be measuring the same aerosols, but not necessarily.

The first of these two methods has been applied only to the observing runs with four or more nights with good extinction determinations and with a good range in the extinction variation in order to be able to define well the slopes of $k_p(\lambda_u)$, $k_p(\lambda_v)$, and $k_p(\lambda_y)$ against $k_p(\lambda_b)$; for example, the Nov'93 observing run had only four nights with complete extinction solutions and these with only a $0\overset{m}{.}023$ range in the "y" extinction coefficient. In contrast the Oct'91 run contained 17 nights with a range of $0\overset{m}{.}072$, and Apr/May'92, 10 nights with a range of $0\overset{m}{.}098$. Also to maintain uniformity, the May'93 run of Ruelas-Mayorga & García-Ruiz (1996) has not been included here. In Figure 9 are shown the $log[k_p(\lambda_i)/k_p(\lambda_b)]$ versus $log[\lambda_i/\lambda_b]$ plots of the seven remaining observing runs. The estimated errors in the derived α_p's range from ± 0.006 to ± 0.15, with the Apr/May'92 run having the smallest error and Mar'93 the largest; a typical error for α_p is ± 0.05. One can clearly detect an evolution of the aerosols in this sequence of graphs.

The $ln[\Delta(extinction)]$ versus $ln[\lambda]$ method has been applied only when the average displacement of the extinction curve above the mean of Table 1 is at least $0\overset{m}{.}05$. In Table 3 is shown the comparison of the α_p values from these two methods. The line "5 May 1992" represents the data from a single night, and so cannot be applied in the $log[k_p(\lambda_i)/k_p(\lambda_b)]$ versus $log[\lambda_i/\lambda_b]$ method; this is the night shown by the "Pinatubo, *uvby* maximum" curve of Fig. 1. For the Oct'91 and Mar'92 observing runs the values for α_p from the two methods are very similar indicating the same aerosols for the "variable" and "displacement" components, whereas the Apr/May'92 and Mar'93 runs show different α_p's arguing for more complex or perhaps bi-modal aerosol distributions, as discussed in many of the above references. Also surprisingly, and as has been noted by other observers such as Sterken & Manfroid (1992) and B95, many of the values for α_p in Table 3 are negative in contrast with what is thought to be a "normal" extinction law for aerosols. B95 and the present study agree well on the α_p values of the volcanic aerosols; both have found flat or moderately negative α_p's for Pinatubo. These negative values point either to a masking of the usual atmospheric opacity components, as we have argued above for the El Chichón extinction curve, and/or a more complex, perhaps bi-modal, extinction law for the volcanic contribution. The trend of the values in Table 3 would suggest an evolution of the average particle size to larger values from Oct'91 through May'92. By Mar'93 and Apr'94 the "variable" component from the $log[k_p(\lambda_i)/k_p(\lambda_b)]$ method had mostly returned to normal with α_p's of the usual meteorological "haze", while the Mar'93 α_p from the "displacement" method is still quite negative indicating large and/or complexly distributed

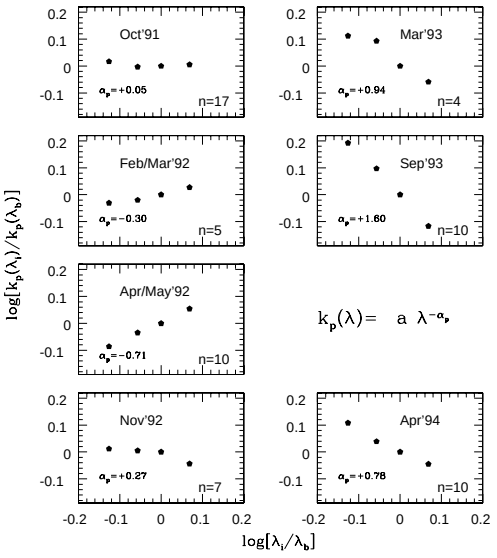

Fig. 9. The log[$k_p(\lambda_i)/k_p(\lambda_b)$] versus log[$\lambda_i/\lambda_b$] plots for seven of the observing periods following the eruption of the Pinatubo volcano. Regressions to the four points of these graphs measure the α_p exponent of the volcanic aerosol extinction law. Within each small graph the number of nights employed and the value of α_p derived are indicated. The values and evolution of these exponents with time give us information concerning the size distributions, evolution, and dispersal of the aerosols from Pinatubo. (See also Table 3.)

particles. The volcanic aerosols were evolving, and at the end of the Pinatubo episode the two methods measured different sized aerosols of different origins. The probable evolution of volcanic aerosols to larger sizes has been noted in many of the above references. By Mar'93 the volcanic aerosols had mostly quit evolving, were dispersing slowly above SPM, and those that remained were mostly the larger sizes, which would slowly fall out of the stratosphere.

5.3. *Episodes of Unusual Atmospheric Extinction*

In Fig. 2 other observing periods show large ranges in the atmospheric extinction values, such as Feb'85 observed by Peña et al. (1998), and May'89 and Apr/May'98 observed by us. These were unaffected by volcanic eruptions but having extinction changes throughout the observing run as large as $\sim 0\overset{m}{.}17$ per air mass in the "y" band. Here our analyses will be dedicated exclusively to the Apr/May'98 period which includes the largest number of extinction determinations for such a period with large non-volcanic variations. Actually this Apr/May'98 period contains two of our observing runs, one from April 20 through May 02, and the other from May 20 through May 29, 1998. The first has the largest extinction changes, from $0\overset{m}{.}124$ to $0\overset{m}{.}293$ per air mass.

The $log[k_p(\lambda_i)/k_p(\lambda_b)]$ method for the variability of the aerosols gives $\alpha_p = 0.284$ for the 10 nights of the "April" run. The other method, $ln[\Delta(extinction)]$ versus $ln[\lambda]$, which measures the displacement of the extinction curve, gives $\alpha_p \sim 0.20$ for the five nights in Apr'98 with the largest extinction values, and ~ 0.15 for the two most extinguished nights, 25/26 Apr'98 and 26/27 Apr'98. All of these values for the "April" run indicate a very flat, almost neutral, extinction change. (See Fig. 5). As discussed above, such changes imply large aerosol particles, larger than the usual meteorological or maritime aerosols normally found above SPM, which give an exponent of $\alpha_p = 0.87$.

A number of sources have been consulted, such as the meteorological data collected at the telescopes, the references of Tapia (1992) and Alvarez & Maisterrena (1977), as well as private discussions with M. Alvarez, C. Chavarria, and D. Hiriart, but it does not seem that a totally clear, unambiguous understanding of the Apr'98 extinction variations can be obtained with the existing, incomplete meteorological data for SPM. Two explanations seem most probable. During the "April" run when the largest extinction variations occurred, most of the wind direction indications were for northerly winds. This is not very usual on SPM. The prevailing winds are from the southwest with generally good "seeing" conditions; see Echevarría et al. (1998). Northerly winds typically bring turbulent conditions and poor "seeing" due to the mountain ranges and variable terrain to the north. So one explanantion for the large extinction variations is that these northerlies have brought unusually large aerosols to SPM, such as urban aerosols from California to the north-northwest, or perhaps desert aerosols from the Santa Clara Valley and Laguna Salada basin to the north-northeast. Such a possibility has already been proposed by S82 based on the 13C data alone, and the expanded graph of the lower right in Fig. 2 would tend to support this interpretation, that a single, abnormal aerosol cloud blew in from the north. A less likely possibility is suggested by the work of Tapia (1992), who shows that April and May are the months with the highest percentages of nights with a high relative humidity. The big aerosols of Apr'98 might have been larger than usual "haze" particles, i.e., meteorological aerosols made up of bigger than usual water droplets due to the higher relative humidities. Measurements made at the 2.1 m telescope during the

critical nights showed relative humidities of 65–83%; relative humidities at the 1.5 m telescope are typically 5–10% higher than those at the 2.1 m due to its somewhat lower altitude.

6. CONCLUSIONS

The main conlusions of this study are the following:

1) The average extinction at SPM, excluding the effects of volcanic outbursts, does not seem to have changed significantly over the period 1973–1999. The mean 13C extinction for the years 1973–1981 has very nearly the same level as the mean 4-color for the years 1987–1999. See Fig. 1 and Table 1.

2) The best months for reliable photometric observations and accuracy are the fall months of September-November when the atmospheric extinction above SPM is more stable and constant for fairly long periods of time, as shown in Figs. 2 and 3. The spring months of March-May may be less stable, with more night-to-night variations, and even suffer extinction peaks, such as for the Apr/May'98 period discussed in § 5.3 and below.

3) A simple 3-component model for the atmospheric extinction of SPM reproduces the extinction curve very well over the wavelengths 3370–6500 Å. Our model includes only Rayleigh-Cabannes and aerosol scatterings plus ozone absorption. For $\lambda > 6500$ Å this model falls short of the observed extinction curve due to the absence of O_2 and H_2O molecular band absorptions.

4) The normal aerosols above SPM are well represented by $k_p(\lambda) = 0.0254\lambda^{-0.87}$, and the final, best model for normal, average conditions above SPM is

$$k(\lambda) = 0.0254\lambda^{-0.87} + 0.0067\lambda^{-4.05} + 0.2581k_{oz}(\lambda),$$

where the $k_{oz}(\lambda)$ values can be estimated from the ozone data of Gast (1961). (See Table 2.)

5) Very clear extinction effects at SPM have been observed due to the stratospheric clouds produced by volcanic eruptions. At SPM the El Chichón and Pinatubo clouds produced very nearly the same maximum increases in the visible extinction, about $0\overset{m}{.}20$ per air mass. However, the spectral distributions and the evolution of the atmospheric extinctions for these two cases were distinct.

6) The 13C extinction observations from Jun'82 through Apr'83 show clear evidence for an evolution and growth of the aerosol particles from El Chichón, as well as indications that the volcanic aerosols mask the usual atmospheric extinction components, such as the Chappuis-band ozone absorptions in the visible and the Rayleigh-Cabannes scattering in the UV.

7) Two analysis methods have been applied to the extinction data for the observing runs affected by the aerosols of the Pinatubo volcano, from Oct'91 through Apr'94. One method, $log[k_p(\lambda_i)/k_p(\lambda_b)]$ versus $log[\lambda_i/\lambda_b]$, measures the variable aerosol component of an observing run, while the other method, $ln[\Delta(extinction)]$ versus $ln[\lambda]$, provides information about the more persistent aerosol component which causes the mean upward displacement of the extinction curve. For some observing runs, such as Mar'92, Apr/May'92, and Mar'93 the aerosol exponents are negative, and for some runs, such as Apr/May'92 and Mar'93 the different methods provide differing α_p's. These values and differences are real since α_p can be measured with an error of about ± 0.05. These unusual results point to a complex, perhaps bimodal, size distribution for the volcanic aerosols.

8) At SPM some observing periods not affected by volcanoes show very large extinction variations from night to night, such as the run of Apr'98. For SPM such behavior occurs mostly during the northern spring (March-May) (see our Fig. 3). Both of our analysis methods indicate large particles for the extinction variations during Apr'98; $\alpha_p \sim 0.15$–0.30. The most plausible explanation is that northerly winds have brought unusual, larger than normal, aerosols from the urban centers to the north-northwest or desert aerosols from the Santa Clara Valley and Laguna Salada basin to the north-northeast.

The authors wish to thank greatly M. Alvarez, C. Chavarría-K., and D. Hiriart for useful discussions concerning the meteorological and observing conditions on SPM, and especially P. E. Nissen for his advice concerning observing and data reduction techniques. We also thank highly C. Chavarría-K., P. E. Nissen, R. B. Stothers, and an un-named referee for careful readings of the final manuscript. Also R. Graef for her continuing secretarial and logistical support, and the librarians M. E. Jiménez and G. Puig for helping us to obtain many source materials used in this study. Many have supported or participated in the observations and data reductions used here, such as J. Guichard, M. E. Contreras-Martínez, A. Franco, A. García-Cole, A. Marquez, M. Ochoa, F. Valera, and G. García, and the technicians and support crews of SPM, such as L. Gutiérrez, V. García, B. Martínez, J. L. Ochoa, J. M. Murillo, J. Valdez, B. Hernández, E. López, and B. García. We are grateful to all of these for their expertise and help. We wish to thank S. González-Bedolla, A. Ruelas-Mayorga, J. H. Peña,

and A. Arellano-Ferro for the use of their extinction data. This work was partially supported over the years by grants from CONACyT (México), Nos. D111-903865, 1219-E9203, 140100G202-006, and 27884E, and DGAPA-UNAM project No. IN101495.

REFERENCES

Allen, C. W. 1963, Astrophysical Quantities, second edition (London: The Athlone Press)

_____. 1973, Astrophysical Quantities, third edition (London: The Athlone Press)

Alvarez, M., & Maisterrena, J. 1977, RevMexAA, 2, 43

Avila, R., Vernin, J., & Cuevas, S. 1998, PASP, 110, 1106

Burki, G., Rufener, F., Burnet, M., Richard, C., Blecha, A., & Bratschi, P. 1995, A&AS, 112, 383 (B95)

Chavarría-K., C., de Lara, E., Finkenzeller, U., Mendoza. E. E., & Ocegueda, J. 1988, A&A, 197, 151

Chavarría-K., C., Terranegra, L., Moreno-Corral, M. A., & de Lara, E. 2000, A&AS, 145, 187

Cox, A. N. 2000, Allen's Astrophysical Quantities, Fourth Edition (New York: Springer)

Echevarría, J., et al. 1998, RevMexAA, 34, 47

Gast, P. R. 1961, in Handbook of Geophysics, revised edition, third printing, U.S. Air Force, Cambridge Research Center, Geophysics Research Directorate (New York: Macmillan) pp.16-1 to 16-32

González-Bedolla, S. 1990, RevMexAA, 21, 401

Grønbech, B., Olsen, E. H., & Strömgren, B. 1976, A&AS, 26, 155

Gutiérrez-Moreno, A., Moreno, H., & Cortés, G. 1982, PASP, 94, 722

Hayes, D.S., & Latham, D. W. 1975, ApJ, 197, 593

Hiriart, D., Goldsmith, P. F., Skrutskie, M. F., & Salas, L. 1997, RevMexAA, 33, 59

Johnson, H. L., Mitchell, R. I., & Latham, A. S. 1967, Comm. Lunar & Planet. Lab., 6, 85

Krueger, A. J. 1983, Sci., 220, 1377

Mendoza V., E. E. 1971, Bol. Obs. Tonantzintla y Tacubaya, 6, 95

Mitchell, R., & Johnson, H. L. 1970, Comm. Lunar & Planet. Lab., 8, 1

Nissen, P. E. 1984, Technical Manual, Description and Data for the Danish 6-channel *uvby-β* Photometer

Parrao, L., Schuster, W. & Arellano-Ferro, A. 1988, Reporte Técnico No. 52, Instituto de Astronomía, UNAM, Mexico City

Peña, J. H., et al. 1998, A&AS, 129, 9

Ruelas-Mayorga, A. & García-Ruiz, G. 1996, RevMexAA, 32, 143

Rufener, F. 1986, A&A, 165, 275

Schuster, W. J. 1982, RevMexAA, 5, 149 (S82)

Schuster, W. J., & Guichard, J. 1985, RevMexAA, 11, 7 (SG)

Schuster, W. J., & Nissen, P. E. 1988, A&AS, 73, 225

Schuster, W. J., Parrao, L., & Contreras-Martínez, M. E. 1993, A&AS, 97, 951

Sterken, C., & Manfroid, J. 1992, A&A, 266, 619

Stothers, R. B. 1997, Journal of Geophys. Research, 102, 6143

_____. 2001, submitted to Journal of Geophys. Research (Atmospheres)

Tapia, M. 1992, RevMexAA, 24, 179

Walker, M. F. 1971, PASP, 83, 401

William J. Schuster: Observatorio Astronómico Nacional, UNAM, Apartado Postal 877, C.P. 22800, Ensenada, B. C., México (schuster@astrosen.unam.mx).

Laura Parrao: Instituto de Astronomía, UNAM, Apartado Postal 70-264, C.P. 04510 México, D. F., México (laura@astroscu.unam.mx).